Quench Protection Study of a Single-Aperture 11 T Nb_3Sn Demonstrator Dipole for LHC Upgrades

G. Chlachidze, N. Andreev, G. Apollinari, B. Auchmann, E. Barzi, R. Bossert, M. Karppinen, F. Nobrega, I. Novitski, L. Rossi, D. Smekens, M. Tartaglia, R. Yamada, and A. V. Zlobin

***Abstract*—The planned upgrade of the Large Hadron Collider (LHC) collimation system will include installation of additional collimators in the dispersion suppressor areas. The longitudinal space for the collimators could be provided by replacing 15-m-long 8.33 T NbTi LHC main dipoles with shorter 11 T Nb_3Sn dipoles compatible with the LHC lattice and main systems. FNAL and CERN have started a joint program with the goal of building a 5.5-m-long twin-aperture Nb_3Sn dipole prototype suitable for installation in the LHC. The first step of this program is the development of a 2-m-long single-aperture demonstrator dipole with a nominal field of 11 T at the LHC nominal current of 11.85 kA. This paper summarizes the results of quench protection studies of 11 T dipoles performed using the single-aperture Nb_3Sn demonstrator.**

***Index Terms*—Accelerator magnets, LHC, magnet quench protection, quench protection heaters, superconducting magnets.**

I. Introduction

THE planned LHC collimation system upgrade will require additional cold collimators in the dispersion suppressor (DS) areas around points 2, 3 and 7, and high luminosity interaction regions 1 and 5 [1]. The space needed for the collimators could be provided by replacing some 15 m long 8.33 T NbTi LHC main dipoles (MB) with shorter 11 T Nb_3Sn dipoles compatible with the LHC lattice and main systems. These twin-aperture dipoles operating at 1.9 K and powered in series with the main dipoles will deliver the same integrated field strength at the nominal LHC current of 11.85 kA.

To demonstrate the feasibility of this approach, CERN and FNAL have begun a joint R&D program with the goal of developing a 5.5 m long twin-aperture Nb_3Sn dipole for the LHC upgrades by 2015 [2]. The program started with the design and construction of a 2 m long 60 mm bore single-aperture demonstrator magnet [3].

Manuscript received October 9, 2012; accepted December 21, 2012. Date of publication January 4, 2013; date of current version February 1, 2013. This work was supported by Fermi Research Alliance, LLC, under Contract DE-AC02-07CH11359 with the US Department of Energy and European Commission under FP7 project HiLumi LHC, GA 284404.

G. Chlachidze, N. Andreev, G. Apollinari, E. Barzi, R. Bossert, F. Nobrega, I. Novitski, M. Tartaglia, R. Yamada, and A. V. Zlobin are with Fermi National Accelerator Laboratory, Batavia, IL 60510 USA (e-mail: guram@fnal.gov; andreev@fnal.gov; apollina@fnal.gov; barzi@fnal.gov; bossert@fnal.gov; nobrega@fnal.gov; novitski@fnal.gov; tartaglia@fnal.gov; yamada@fnal.gov; zlobin@fnal.gov).

B. Auchmann, M. Karppinen, L. Rossi, and D. Smekens are with the European Organization for Nuclear Research, CERN CH-1211, Geneve 23, Switzerland (e-mail: bernhard.auchmann@cern.ch; Mikko.Karppinen@cern.ch; Lucio.Rossi@cern.ch; david.smekens@cern.ch).

Color versions of one or more of the figures in this paper are available online at http://ieeexplore.ieee.org.

Digital Object Identifier 10.1109/TASC.2013.2237871

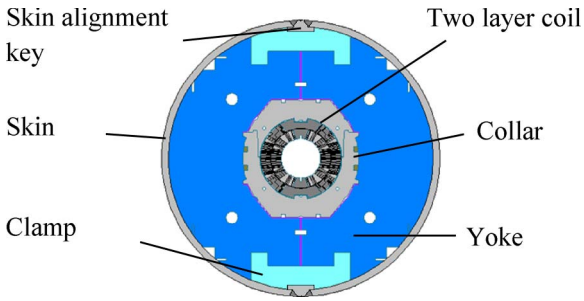

Fig. 1. Cold-mass cross-section.

Quench protection of the 11 T dipoles will be provided by protection heaters. This paper briefly describes the magnet design and protection heater parameters used in the 2 m long demonstrator dipole, and presents the first experimental results of quench protection studies. Magnet quench performance and magnetic measurements are reported in [4], [5].

II. Magnet and Heater Design

Details of the 11 T demonstrator dipole design are reported in [3]. Fig. 1 shows the cold mass cross-section.

The coil consists of 56 turns—22 in the inner layer and 34 in the outer layer. Each coil is wound using 40 strand Rutherford cable [6] insulated with two layers of E-glass tape, each 0.075 mm thick and 12.7 mm wide. The cable is made of 0.7 mm diameter Nb_3Sn RRP-108/127 strand with a nominal J_c (12 T, 4.2 K) of 2750 A/mm^2 (without self-field correction), a Cu fraction of 0.53, and RRR above 60.

The coils are surrounded by ground insulation made of 5 layers of 0.127 mm thick Kapton film with quench heaters between the Kapton layers (Fig. 2), stainless steel protection shells and laminated collars. The collared coil assembly is placed inside two half-yokes locked with aluminum clamps. The stainless steel (SS) skin is welded to obtain a coil pre-stress sufficient to keep it under compression up to the full design field of 12 T. Two thick stainless steel end plates welded to the skin restrict the axial coil motion due to the Lorentz forces. The details of magnet fabrication are reported in [4], [7].

The magnet quench protection heaters are composed of 0.025 mm thick stainless steel strips, 21 mm wide at the mid-plane blocks and 26 mm wide at the pole blocks. Two strips connected in series are inserted between the ground insulation layers and placed on the outer surface of the coil blocks (Fig. 2). Each coil has two protection heaters marked as PH-1L and PH-2L. PH-1L is installed between the 1st and 2nd Kapton

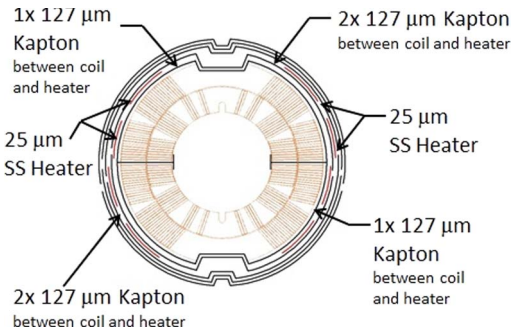

Fig. 2. Ground insulation and protection heater position.

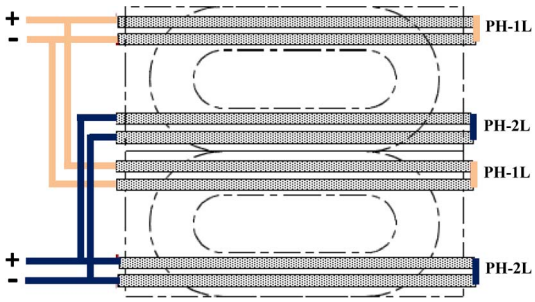

Fig. 3. Heater connection scheme.

TABLE I
DEMONSTRATOR DIPOLE QUENCH PROTECTION PARAMETERS

Parameter	Value
Magnet inductance at I_{nom}	6.04 mH/m
Stored energy at I_{nom}	424 kJ/m
Energy density in coil at I_{nom}	85.9 MJ/m^3
Effective coil length	1.7 m
Short sample current/field at 1.9 K	15.0 kA/13.4 T
Stored energy at I_{max}=15 kA	680 kJ/m

layers on one side of the coil and PH-2L—between the 2nd and 3rd Kapton layers on the other coil side.

The corresponding protection heaters on each coil are connected in parallel forming two heater circuits (Fig. 3). Each pair of protection heaters covers 31 turns (15 in the mid-plane and 16 in the pole block) per quadrant or ∼55% of the total outer coil surface. The resistance of each protection heater measured at room temperature is 5.9 ohms and about 4.2 ohms at 4.5 K.

III. QUENCH PROTECTION PARAMETERS

The quench protection parameters of the 11 T demonstrator dipole at the LHC nominal current of 11.85 kA are summarized in Table I.

The maximum coil temperature T_{max} after a quench in adiabatic conditions is determined by the equation:

$$\int_0^{\infty} I^2(t)dt = \lambda \cdot S^2 \cdot \int_{Tq}^{T_{max}} \frac{C(T)}{\rho(T)}dt \qquad (1)$$

where $I(t)$ is the current decay after a quench (A); T_q is the conductor quench temperature (K); S is the cross-section of the insulated cable (m^2); λ is fraction of Cu in the insulated cable

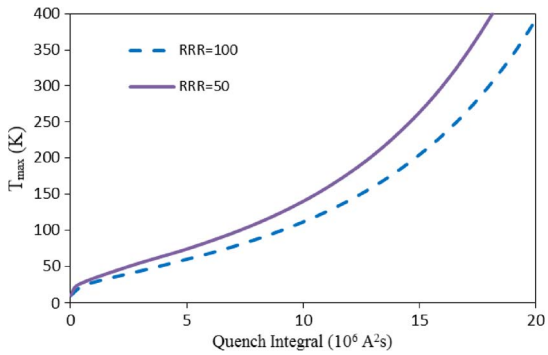

Fig. 4. Cable maximum temperature $T_{\max}$ versus quench integral for the insulated and epoxy-impregnated cable.

cross-section; $C(T)$ is the average specific heat of the insulated cable $(\mathrm{J} \cdot \mathrm{K}^{-1} \cdot \mathrm{m}^{-3})$; $\rho(T)$ is the cable resistivity $(\mathrm{ohm} \cdot \mathrm{m})$.

The dependence of T_{max} on the value of quench integral (QI) calculated for the demonstrator dipole cable insulated with E-glass tape and impregnated with epoxy for two values of cable RRR is shown in Fig. 4.

To keep the cable temperature during a quench below 400 K, the quench integral has to be less than 18–20 MIITs $(10^6\ \mathrm{A}^2\mathrm{s})$. This criterion for a maximum cable temperature (still under discussion) is considered currently as a safe limit for Nb_3Sn accelerator magnets [8].

The maximum value of the quench integral in the turn where the quench originated is determined by the equation:

$$\int_0^{\infty} I^2(t)dt = I_0^2 \cdot \tau_D + \int_{\tau_D}^{\infty} I^2(t)dt \qquad (2)$$

where I_o is the magnet current when the quench started; τ_D is the total delay time including the quench detection, protection switch operation and heater delay time; and $I(t)$ is the current decay in the magnet after the protection heaters were fired.

IV. PROTECTION HEATER STUDY

Protection heater parameters such as heater delay time (the time between the heater ignition and the start of quench development in the coil) and coil volume under the protection heaters as well as quench propagation velocity in the coil provide significant impact on τ_D and $I(t)$ in (2) and thus on the value of the maximum temperature in the quench origin area. Experimental study of these parameters for the 11 T demonstrator dipole is the main goal of this work.

Temperature profiles in the demonstrator dipole after a heater-induced quench, simulated using ANSYS-based code [9], are shown in Fig. 5. The left diagram corresponds to the moment when a heater-induced quench starts in the outer-layer turns under the heater. The right diagram illustrates quench propagation in the azimuthal and radial directions in the magnet and provides information on quench propagation time inside the coil.

The first simulations of heater-induced quenches in the demonstrator dipole revealed that quenches in Nb_3Sn coils propagate radially rather quickly between two layers [10].

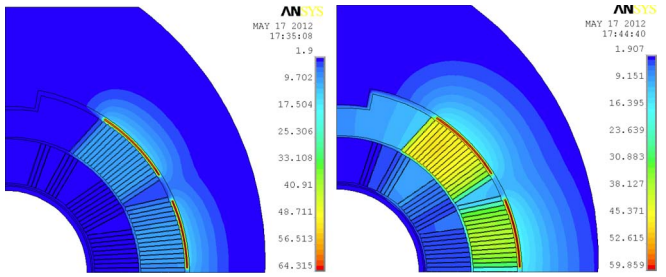

Fig. 5. Temperature profile in the demonstrator magnet after ~50 ms (left) and ~100 ms (right) from the heater discharge

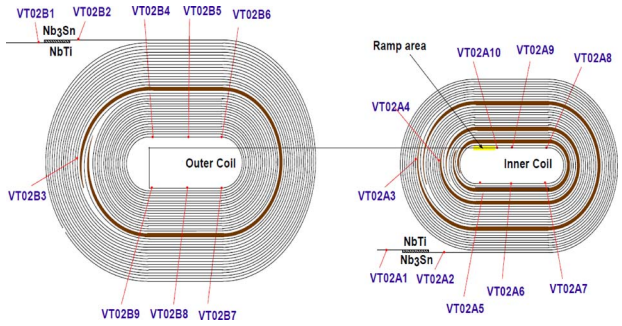

Fig. 6. Voltage tap scheme in the 11 T demonstrator dipole coil.

This observation was also experimentally verified during the protection heater tests in the demonstrator dipole.

V. Test Results

The 11 T demonstrator dipole was tested at FNAL Vertical Magnet Test Facility [11]. The coils were instrumented with voltage taps for quench detection and localization. The voltage tap system covers the pole turn, multi-turn and splice sections of the inner and outer coil layers of both coils. The voltage tap scheme for one of the coils is shown in Fig. 6. Voltage taps in pole turn allow measuring quench propagation velocity in the case of spontaneous quenches in this area. Voltage taps on each current block provide the quench propagation time between these blocks.

A. Protection Heater Study

A series of tests was performed to evaluate the efficiency of the heaters with different insulation (PH-1L and PH-2L) and the ability to quench the coil with a reasonably short delay time. Heater delay time was defined as the time between the heater ignition and the start of quench development in the coil. For every test, a pair of heaters with a specific insulation was fired while another pair of heaters were used for the magnet protection along with the stored energy extraction system. Due to limited quench performance [4], heater tests were performed only at magnet currents up to 65% of the estimated short sample limit (SSL). The energy extraction circuit delay was 1 ms for all heater tests except for the radial quench propagation study, when the extraction dump was delayed for 120 ms.

Heater delay time as a function of the peak heater power dissipated in the magnet at 4.5 K is shown in Fig. 7. The peak heater power per heater area is defined as $I_{\mathrm{PH}}^2 \cdot R_{\mathrm{PH}}/A$, where

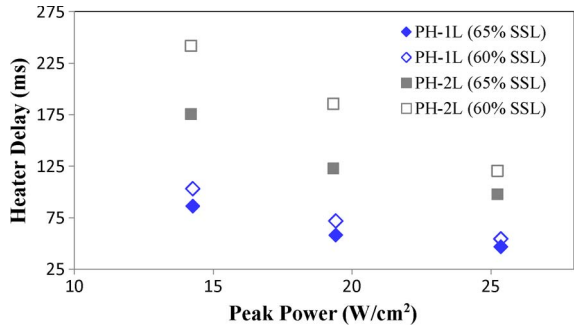

Fig. 7. Heater delay as a function of peak dissipated power at 4.5 K.

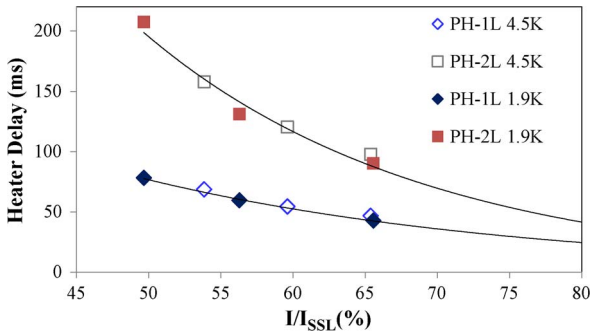

Fig. 8. Heater delay at a different SSL ratio.

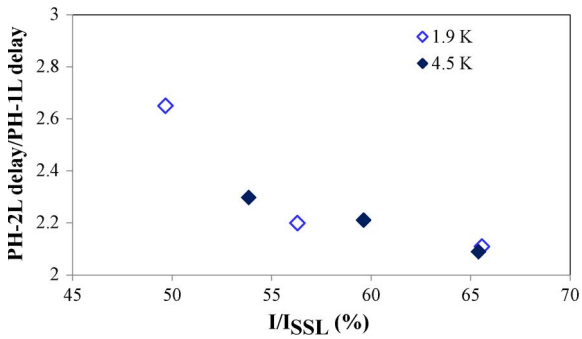

Fig. 9. Effect of coil current on heater efficiency.

I_{PH} is the maximum heater current (A), R_{PH} and A are the heater resistance (ohm) and area (cm^2) respectively. The data are shown at magnet currents corresponding to 60% and 65% of SSL at 4.5 K. Changing the heater power by almost a factor of 2 proportionally reduces the heater delay time for both heaters.

Heater delay at a different SSL ratio (I/I_{SSL}) measured both at 4.5 K and 1.9 K is shown in Fig. 8. One can notice that the heater delay time practically is not dependent upon magnet operation temperature but strongly dependent upon heater insulation thickness. Extrapolation of the measurement data to the nominal operation current (80% of SSL) gives ~25 ms and ~40 ms heater delay time for PH-1L and PH-2L respectively. The corresponding extrapolated values at the injection current (5% of SSL) are ~420 ms and ~2000 ms. The delay time of PH-2L both at low and high currents is unacceptably large.

The delay time ratio of PH-2L and PH-1L as a function of the magnet current is shown in Fig. 9. The peak dissipated power in these tests was 25 W/cm^2, and the decay time constant (RC) of the heater circuit was set to 25 ms. One can see that PH-1L with

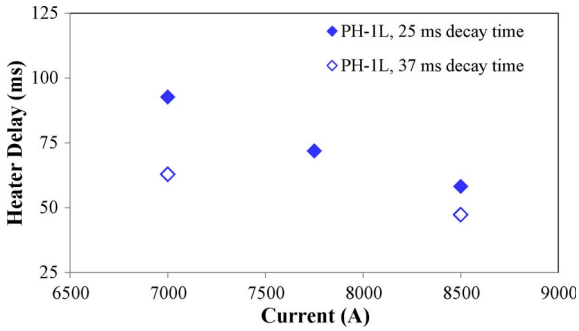

Fig. 10. Heater delay as a function of magnet current for the peak heater power of $\sim$ 20 W/cm^2 and different decay time constant of the heater circuit.

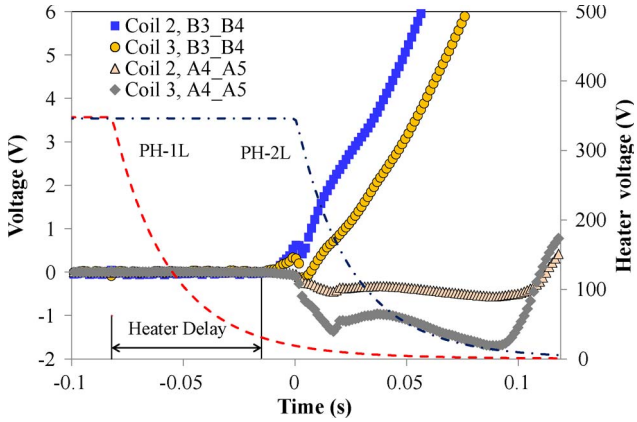

Fig. 11. PH-1L heater-induced quench with a dump delay of 120 ms. Quench developed in 65 ms after heater ignition (PH-1L heater delay). PH-2L heaters are fired at the moment of quench detection ($t = 0$ ms).

a single layer of 0.127 mm thick Kapton insulation exhibited significantly shorter delay time than PH-2L with two layers of 0.127 mm thick Kapton insulation, especially at low currents. Note that at high currents the ratio of the Kapton insulation thickness of PH-2L to PH-1L is approaching two.

Heater delays could be further reduced by increasing the decay time constant of the heater circuit at the same peak heater power (Fig. 10).

B. Radial Quench Propagation

To observe the quench propagation from the outer to the inner coil layer in heater-induced quenches at 4.5 K, the extraction dump was delayed for 120 ms. A quench at a magnet current of 8 kA ($\sim$62% of SSL) was provoked by igniting PH-1L while PH-2L was used for the magnet protection.

Fig. 11 shows the development of the resistive voltage signal in the outer and inner coil layers. The heater voltage discharge both in PH-1L and PH-2L is also shown in Fig. 11. After $\sim$65 ms of the PH-1L ignition, a quench was initiated in the pole block of the outer coil layer (segment $B3\_B4$ in Fig. 6). After an additional $\sim$85 ms, clear resistive signals appeared in the inner coil layer segments $A4\_A5$ and $A3\_A4$ (not shown in Fig. 11). This experiment clearly confirms the rapid quench propagation from outer to inner layers in Nb_3Sn accelerator magnets predicted by simulations in [10]. Based on Fig. 8, the coil response on PH-2L ignition (even with possible quench-back) is delayed for $\sim$120 ms at 62% of SSL and thus does not affect the quench development in the inner coil layer shown in Fig. 11.

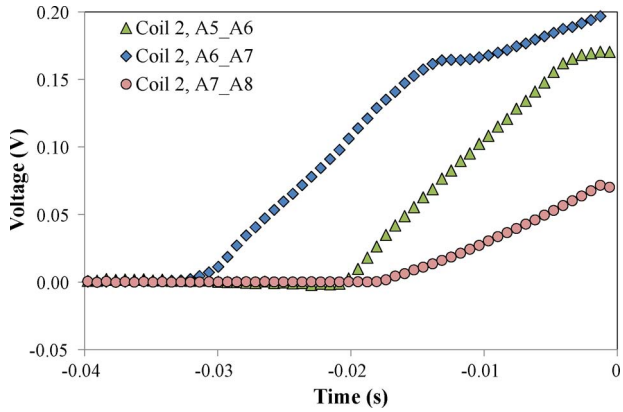

Fig. 12. Quench onset for the ramp where the quench propagation speed was measured in an inner-layer pole turn.

C. Longitudinal Quench Propagation

Most of the training quenches started in the mid-plane area of the outer coil layer and only a few quenches occurred in the inner-layer pole-turn segments with high magnetic field [4]. The longitudinal quench propagation velocity was measured in one of the quenches in the inner-layer pole turn at 4.5 K using the time-of-flight method as $\sim$27 m/s (see quench onset in Fig. 12). Quench current in this ramp was 9440 A, which corresponds to $\sim$73% of SSL at 4.5 K.

The measured value of the longitudinal quench propagation velocity is comparable or higher than results obtained for other Nb_3Sn magnets [12], [13]. Measurements of quench propagation velocity will continue on the next models with improved quench performance and coil instrumentation (spot heaters and additional voltage taps).

VI. Conclusion

Protection heaters with 0.127 mm and 0.254 mm Kapton insulation thickness were evaluated for the 11 T dipole. The results of the study show acceptable heater efficiency and delay times for the heater with a single 0.127 mm thick Kapton film. This heater design will be used in the next 11 T dipole models. Fast quench propagation between the outer and inner coil layers was experimentally observed for the heater-induced quench. Longitudinal quench propagation velocity in pole turn at $\sim$73% of SSL was also measured. Due to limited magnet performance, heater tests were performed only at magnet currents up to 65% of SSL. Quench protection studies will continue with improved 11 T dipole models.

Acknowledgment

The authors thank the technical staff of FNAL Technical Division for contributions to magnet design, fabrication and test.

REFERENCES

[1] L. Bottura *et al.*, "Advanced accelerator magnets for upgrading the LHC," *IEEE Trans. Appl. Supercond.*, vol. 22, no. 3, p. 4002008, 2012.

[2] A. V. Zlobin *et al.*, "Development of Nb_3Sn 11 T single aperture demonstrator dipole for LHC upgrades," in *Proc. PAC*, NYC, 2011, p. 1460.

[3] A. V. Zlobin *et al.*, "Design and fabrication of a single-aperture 11 T Nb_3Sn dipole model for LHC upgrades," *IEEE Trans. Appl. Supercond.*, vol. 22, no. 3, p. 4001705, 2012.

[4] A. V. Zlobin *et al.*, "Development and test of a single-aperture 11 T Nb_3Sn demonstrator dipole for LHC upgrades," *IEEE Trans. Appl. Supercond.,* doi:10.1109/TASC.2012.2236138.

[5] N. Andreev *et al.*, "Field Quality Measurements in a Single-Aperture 11 T Nb_3Sn Demonstrator Dipole for LHC Upgrades," *IEEE Trans. Appl. Supercond.,* doi:10.1109/TASC.2013.2237819.

[6] E. Barzi *et al.*, "Development and fabrication of Nb_3Sn rutherford cable for the 11 T DS dipole demonstration model," *IEEE Trans. Appl. Supercond.*, vol. 22, no. 3, p. 6000805, 2012.

[7] A. V. Zlobin *et al.*, "Status of a single-aperture 11 T Nb_3Sn demonstrator dipole for LHC upgrades," in *Proc. IPAC*, 2012, pp. 1098–1100.

[8] G. Ambrosio *et al.*, "LARP long Nb_3Sn quadrupole design," *IEEE Trans. Appl. Supercond.*, vol. 18, no. 2, p. 268, 2008.

[9] R. Yamada *et al.*, "2D/3D quench simulation using ansys for epoxy impregnated high field magnets," *IEEE Trans. Appl. Supercond.*, vol. 3, no. 3, pp. 1696–1699, 2003.

[10] A. V. Zlobin, I. Novitski, and R. Yamada, "Quench protection analysis of a single-aperture 11 T Nb_3Sn demonstrator dipole for LHC upgrades," in *Proc. IPAC*, 2012, pp. 3599–3601.

[11] M. J. Lamm *et al.*, "A new facility to test superconducting accelerator magnets," in *Proc. PAC*, 1997, pp. 3395–3397.

[12] TD-05-030 S. Feher *et al.*, "HFDM4 test summary," Fermilab Technical Notes, Apr. 2005 TD-05-030.

[13] M. Marchevsky *et al.*, "Quench performance of HQ01, a 120 mm bore LARP quadrupole for the LHC upgrade," *IEEE Trans. Appl. Supercond.*, vol. 22, no. 3, p. 4702005, 2012.